

Liposomes coated with *N*-trimethyl chitosan to improve the absorption of harmine in vivo and in vitro

Wei-liang Chen^{1,*}Zhi-Qiang Yuan^{1,*}Yang Liu¹Shu-di Yang¹Chun-ge Zhang¹Ji-zhao Li¹Wen-jing Zhu¹Fang Li¹Xiao-feng Zhou^{2,3}Yi-mei Lin⁴Xue-nong Zhang¹

¹Department of Pharmaceutics, College of Pharmaceutical Sciences,

²Department of Radiobiology, College of Radiological Medicine and Protection, Soochow University, Suzhou, ³Changshu Hospital of Traditional Chinese Medicine, Changshu, ⁴The Second Affiliated Hospital of Xinjiang Medical University, Urumqi, People's Republic of China

*These authors contributed equally to this work

Abstract: In this study, harmine liposomes (HM-lip) were prepared through the thin-film hydration–pH-gradient method and then coated with *N*-trimethyl chitosan (TMC). Particle size, zeta potential, entrapment efficiency, and in vitro release of HM-lip and TMC-coated harmine liposomes (TMC-HM-lip) were also determined. Sprague Dawley rats were further used to investigate the pharmacokinetics in vivo. Retention behavior in mouse gastrointestinal tract (GIT) was studied through high-performance liquid chromatography and near-infrared imaging. Degradation was further evaluated through incubation with Caco-2 cell homogenates, and a Caco-2 monolayer cell model was used to investigate the uptake and transport of drugs. HM-lip and TMC-HM-lip with particle size of 150–170 nm, an entrapment efficiency of about 81%, and a zeta potential of negative and positive, respectively, were prepared. The release of HM from HM-lip and TMC-HM-lip was slower than that from HM solution and was sensitive to pH. TMC-HM-lip exhibited higher oral bioavailability and had prolonged retention time in GIT. HM-lip and TMC-HM-lip could also protect HM against degradation in Caco-2 cell homogenates. The uptake amount of TMC-HM-lip was higher than that of HM and HM-lip. TMC-HM-lip further demonstrated higher apparent permeability coefficient (P_{app}) from the apical to the basolateral side than HM and HM-lip because of its higher uptake and capability to open tight junctions in the cell monolayers. TMC-HM-lip can prolong the retention time in the GIT, protect HM against enzyme degradation, and improve transport across Caco-2 cell monolayers, thus enhancing the oral bioavailability of HM.

Keywords: harmine, liposomes, TMC, bioavailability, Caco-2 cell

Introduction

Oral administration has considerably developed because of its advantages over injection administration. Oral administration is widely accepted by patients because it is painless, and it improves patient compliance. However, an orally administered drug exhibits unsatisfactory bioavailability because it encounters many barriers. On one hand, a drug may not be efficiently absorbed because of its low solubility, low permeability, or efflux effect of p-glycoprotein (p-gp) in intestines.¹ On the other hand, degradation by the enzymes secreted in intestines can also destroy the drug before it enters into the blood circulation.² To overcome these obstacles, scholars have investigated various approaches, such as the use of permeability enhancers, p-gp inhibitors, or enzyme inhibitors, but obtained unsatisfactory results.³

Nanocarriers, such as liposomes, micelles, and nanoparticles, have gained considerable attention in the field of oral administration, because they can improve the bioavailability of orally administered drugs.⁴ Liposomes containing phospholipids and cholesterol can protect encapsulated drugs against enzyme degradation by the

Correspondence: Xue-nong Zhang
Department of Pharmaceutics, College of Pharmaceutical Sciences, Soochow University, DuShuHu High Education Zone, Su Zhou 215123, Jiang Su Province, People's Republic of China
Tel +86 512 6588 2087
Fax +86 512 6588 2087
Email zhangxuenong@163.com

enzymes in the gastrointestinal tract (GIT) and reduce the first-pass effect.⁵ Encapsulated drugs must be gradually released from liposomes to prolong their residence time in the GIT. Various studies showed that liposomes can enhance the absorption of encapsulated drugs by intestinal epithelial cells through endocytosis, and thus improve the bioavailability.⁶ However, the stability of liposomes is not good as they may be damaged in gastric fluid and result in the rapid release of the encapsulated drugs. Therefore, polymers such as chitosan (CS) have been used to coat liposomes and improve their stability *in vitro* and *in vivo*.⁷

CS, a pyran polysaccharide deacetylated from chitin, exhibits good biocompatibility, biodegradability, and nontoxicity. CS has been widely used to prepare nanocarriers such as micelles and nanoparticles.⁸ Nanoparticles based on CS and its derivatives, such as *N*-trimethyl CS (TMC), could enhance the oral bioavailability of encapsulated drugs by opening tight junctions in intestinal epithelial cells.⁹ Coating of anionic liposomes with CS and its derivatives via electrical attraction may result in charge reversal on their surface.¹⁰ Liposomes coated with CS or TMC maintain the capability to open tight junctions, improve absorption, and further prolong the residence time in GIT,¹¹ and thus enhance the oral bioavailability.

Nowadays, Caco-2 cell monolayers have been widely used to study the absorption, cellular uptake, cytotoxicity, and metabolism and evaluate the behavior of oral drugs in intestines. Caco-2 cells are derived from human colon adenocarcinoma cells and can differentiate into cells *in vitro* similar to that of intestinal cells. The coexistence of enzymes and p-gp in Caco-2 cells is important for the evaluation of metabolism and efflux effect of oral drugs.¹²

Harmine (HM), derived from *Peganum harmala*, is a β -carboline compound that exhibits antitumor effect.¹³ In this study, HM was encapsulated into liposomes and then coated with TMC. The pharmacokinetics of HM, HM-liposomes (HM-lip), and TMC-HM-lip in rats was studied by determining HM concentration in plasma after oral administration. To elucidate “double peaks” in the blood concentration curve after the oral administration of HM-lip and TMC-HM-lip, the residence time in GIT was investigated through high-performance liquid chromatography (HPLC) and near-infrared (NIR) imaging. The uptake and transport across Caco-2 cell monolayers were also assessed to promote the absorption mechanism of liposomes coated with TMC.

Materials

CS (molecular weight [MW] of 8–10 kDa, deacetylation degree 93.1%) was purchased from Xingcheng Biochemical

Co, Ltd (Nantong, People’s Republic of China). TMC was synthesized in our laboratory with a quaternization degree of 65%¹⁴ and an average MW of 6.5 kD.

Dulbecco’s Modified Eagle’s Medium was provided by Hyclone (GE Healthcare Bio-Sciences Corp., Piscataway, NJ, USA). Fetal bovine serum, nonessential amino acids, and penicillin–streptomycin were purchased from Gibco (Grand Island, New York, NY, USA). All other reagents and solvents were of analytical grade and were commercially available.

Caco-2 cells were obtained from Fu Dan University (Shanghai, People’s Republic of China). Sprague Dawley rats weighing 250–300 g and Kunming mice with weights ranging from 18 to 22 g were provided by the Experimental Animal Center, Soochow University (Suzhou, People’s Republic of China). Female nude mice 4–6 weeks old were also provided by the same Experimental Animal Center. All animals were kept in an environment complying with the National Institutes of Health Guidelines for the care and use of laboratory animals. All animal procedures were performed following protocol approval by the Medical Ethics Committee of Soochow University.

Methods

Preparation, characterization, and *in vitro* release of HM-lip and TMC-HM-lip

Preparation of HM-lip and TMC-HM-lip

HM-lip was prepared through thin-film hydration according to the method reported by Guo et al¹⁵ with some modifications. Briefly, SPC/chol/HM (20/5/4, w/w) were dissolved in chloroform and dried through rotary evaporation at 37°C to form a thin film. The organic solvent was completely removed by drying under vacuum. The thin film was hydrated with 20 mL of 50 mM citric acid with shaking and mixing. To obtain high encapsulation efficiency, the pH of the suspension was adjusted to 6.8 with 50 mM Na₂CO₃. Liposomes with smaller particle sizes were obtained following probe sonication for 10 minutes.

An aliquot of HM-lip was mixed with the same volume of TMC (0.1%) in PBS (phosphate-buffered saline; pH 6.8) and then incubated at 4°C for 1 hour to prepare TMC-HM-lip.

Characterization of HM-lip and TMC-HM-lip

The particle sizes and zeta potentials of HM-lip and TMC-HM-lip were measured with a Zetamaster 3000H instrument (Malvern Instruments, Malvern, UK). The surface morphologies of HM-lip and TMC-HM-lip were viewed using an H-7000 model transmission electron microscope (Hitachi, Tokyo, Japan).

The entrapment efficiencies of HM-lip and TMC-HM-lip were determined through ultracentrifugation method at $20,000\times g$ and 4°C for 45 minutes. The amount of free drug in the supernatant was measured through HPLC under the following conditions: ODS column (GL Science, Torrance, CA, USA), mobile phase = methanol: 0.01 M $(\text{NH}_4)_2\text{SO}_4$: triethylamine solution (adjusted to pH 3.8 with phosphate) (60:40:0.6, v/v), flow rate = 1 mL/min, injection volume = 20 μL , and wavelength = 220 nm.¹⁶ Total drug in the suspension was determined by mixing HM-lip or TMC-HM-lip with methanol and then measured using HPLC. Entrapment efficiency was calculated using the following equation:

$$\text{EE \%} = \frac{\text{Weight of encapsulated drug}}{\text{Weight of total drug}} \times 100\% \quad (1)$$

Release of HM from HM-lip and TMC-HM-lip in vitro

The release of HM from HM-lip and TMC-HM-lip was investigated through dialysis method. Briefly, 2 mL of HM-lip, TMC-HM-lip, and HM (dissolved in pH 6.8 PBS, 2 mg/mL) solutions were loaded into a dialysis tube (MWCO = 8,000). The dialysis tubes were immersed into 50 mL of release medium (0.1 mol/L HCl or pH 5.3, 6.8, and 7.4 PBS) and incubated in a constant temperature shaker at 37°C with a speed of 100 rpm. Samples (1 mL) were obtained at the predetermined time points and replaced with an equal volume of fresh medium. The concentration of HM in the release medium was measured using HPLC.

In vivo pharmacokinetic studies

Prior to experiment, SD rats were fasted for 24 hours and given free access to water. These rats were divided into four groups ($n=6$ per each group). HM, HM-lip, and TMC-HM-lip solutions (60 mg/kg) were intragastrically given to rats in groups 1–3, respectively. About 0.5 mL of blood samples was obtained from the femoral artery at predetermined time points. The blood samples were centrifuged at 1,000 rpm for 10 minutes to separate the blood cells from plasma. Briefly, 10 μL of tinidazole (100 $\mu\text{g}/\text{mL}$) was added to 0.2 mL of the plasma and set as the internal standard. The sample was alkalized with 1 mL of saturated Na_2CO_3 solution and extracted with 5 mL of ethyl acetate. Ethyl acetate was dried in a water bath (80°C) and 0.2 mL of methanol was added to dissolve the residue. About 20 μL of methanol was measured through HPLC with the conditions as described in the “Characterization of HM-lip and

TMC-HM-lip” section. For comparison, the rats in group 4 were intravenously given an HM solution (20 mg/kg), and plasma HM was then measured.

Pharmacokinetic data were analyzed using the 3P97 software or origin 8.0. The peak concentration (C_{max}) and the time consumed by HM to reach peak concentration (T_{max}) in the plasma were obtained by 3P97 or through visual inspection from the concentration–time curve. The area under the concentration–time curve (AUC_{0-t}) was calculated with 3P97 or origin 8.0.

Retentive behavior of HM-lip and TMC-HM-lip in GIT

The retentive behavior of HM-lip and TMC-HM-lip in the GIT of mice was evaluated using the method of Takeuchi et al¹⁷ with some modifications. Briefly, mice were separated into three groups and fasted for 24 hours before the test. Mice in groups 1–3 were given HM, HM-lip, and TMC-HM-lip (60 mg/kg), respectively. Three mice from each group were sacrificed, and their GITs were homogenized with 2 mL of methanol without washing at the predetermined time points. The homogenized suspension was centrifuged at 1,000 rpm for 10 minutes, and 1 mL of methanol in the supernatant was taken out. Methanol was dried in a water bath (80°C) and 0.2 mL of methanol was then added to dissolve the residue. The amount of drug in methanol was measured to obtain the residual amount of HM, HM-lip, and TMC-HM-lip in the GIT of mice.

Dir-loaded liposomes (Dir-lip) and Dir-loaded liposomes coated with TMC (TMC-Dir-lip) were used to determine the retentive behavior in the GIT of mice. Dir-lip and TMC-Dir-lip were prepared using the method described in the “Preparation of HM-lip and TMC-HM-lip” section with some modifications. Briefly, Dir-lip was prepared through thin-film hydration method without the pH-gradient method. TMC-HM-lip was obtained by coating Dir-lip with TMC (0.1%). The final concentration of Dir in Dir-lip and TMC-Dir-lip was 20 $\mu\text{g}/\text{mL}$. The concentration of lipids in Dir-lip and TMC-Dir-lip was similar to that in HM-lip and TMC-HM-lip.

Retentive behavior test was performed through NIR imaging. Nude mice fasted for 24 hours were orally administered with Dir-lip and TMC-Dir-lip. At the predetermined time points (2, 4, 6, 8, 12, and 24 hours) after administration, the fluorescent distribution was imaged with an in vivo imaging system at the wavelengths of λ_{ex} 720 nm and λ_{em} 790 nm (IVIS Lumina II; Caliper Life Sciences, Hopkinton, MA, USA).¹⁸

Toxicity of HM, HM-lip, and TMC-HM-lip to Caco-2 cells

The toxicity of HM, HM-lip, and TMC-HM-lip against Caco-2 cells was evaluated using the MTT cytotoxicity assay reported by Lin et al¹⁹ with some modifications. Briefly, Caco-2 cells were seeded in 96-well plates at a cell density of 2×10^4 cells/well and incubated for 5 days before the test. The cells were incubated with cell medium replaced by different concentrations of HM, HM-lip, or TMC-HM-lip solution for 24 hours. Each well has 20 μ L of MTT (5 mg/mL in PBS) added and then incubated for another 4 hours. The solution in each well was removed with 100 μ L of dimethyl sulfoxide. Absorbance was determined through enzyme immunoassay at 570 nm, and cell viability was calculated using the following equation:

$$\text{Cell viability (\%)} = \frac{A_{\text{treated}} - A_0}{A_{\text{notreated}} - A_{\text{treated}}} \times 100\% \quad (2)$$

where A_{treated} is the absorbance of the well treated with HM, HM-lip, or TMC-HM-lip. A_0 is the absorbance of the well with no cells, and $A_{\text{notreated}}$ is the absorbance of the well treated with blank medium.

Degradation of HM, HM-lip, and TMC-HM-lip in Caco-2 cell homogenates

The degradation of HM, HM-lip, and TMC-HM-lip in Caco-2 cell homogenates was determined using the method of Li et al²⁰ with some modifications. Caco-2 cells grown for 14 days were collected and mixed with 5 mL of ice-cold PBS. The cells were homogenized with a probe sonicator for 1 minute. Caco-2 cell homogenates were obtained through centrifugation of the suspension at $8,000 \times g$ for 10 minutes at 4°C , and supernatant was collected. Degradation was tested by mixing the cell homogenates with the same volume of HM, HM-lip, or TMC-HM-lip solution and then incubated at 37°C . At each predetermined time point, 0.1 mL of sample was obtained and mixed with 0.9 mL of methanol to terminate the reaction. The sample was centrifuged at 3,000 rpm, and the concentration of HM in each sample was measured through HPLC.

Uptake studies

The amounts of HM, HM-lip, and TMC-HM-lip absorbed by Caco-2 cells were determined using the method reported by Guan et al²¹ with some modifications. Briefly, Caco-2 cells were seeded in 6-well plates at 1×10^5 cells/cm² and cultured for 15 days before the studies. On day 15, the medium was

removed and Caco-2 cell monolayers were washed twice with PBS. The cell monolayers were incubated with 2 mL of PBS (with or without NaN_3 , CyA, or CPZ) for 15 minutes. Preincubation was terminated, and PBS was replaced by 2 mL of the preincubated drug solution (HM, HM-lip, or TMC-HM-lip). The cells were washed with cold PBS three times after the incubation at predetermined time points. The cells were then removed using a cell scraper and homogenized with a probe sonicator for 1 minute. Around 1 mL of the homogenate was mixed with the same volume of methanol and then centrifuged at 3,000 rpm for 10 minutes to precipitate the proteins. The concentration of HM was measured through HPLC, and the uptake amount of HM into Caco-2 cells was determined. Protein content was also measured according to Bradford's method.

Transport of HM, HM-lip, and TMC-HM-lip across Caco-2 cell monolayers

Caco-2 cells were seeded onto a permeable polycarbonate insert (1.1 cm², 1 μ m pore size) (Millipore, Billerica, MA, USA) at 1×10^5 cells/cm² and the insert was placed in 12-well tissue culture plates (Corning Inc, Corning, NY, USA). The cells were cultured for 21 days, and the integrity of the monolayers was assessed by measuring the transepithelial electrical resistance (TEER) of the monolayers and phenol red transport before the transport test.

The transport test across Caco-2 cells was performed using the method reported by Guan et al²¹ with some modifications. The Caco-2 cell monolayers were washed with the incubation medium twice after removing the culture medium. The monolayers were then preincubated with 0.5 and 1.5 mL of the incubation medium on the apical and basolateral sides, respectively, for 15 minutes at 37°C . The incubation medium was removed. About 0.5 mL of the incubation medium containing HM, HM-lip, or TMC-HM-lip was added to the apical side, and 1.5 mL of the unmodified incubation medium was added to the basolateral side to study the transport from the apical side to the basolateral side. The Caco-2 cell monolayers were incubated in an incubator at 37°C . Then, 0.05 mL of the sample was obtained from the basolateral side at 10, 30, 60, and 120 minutes, and the same volume of fresh incubation medium was added. For the study of transport from the basolateral side to the apical side, 1.5 mL of the incubation medium containing HM, HM-lip, or TMC-HM-lip and 0.5 mL of the unmodified incubation medium were added to the opposite side. Samples were obtained from the apical side.

The HM concentration in each sample was measured through HPLC as described in the "Characterization of

Table 1 Characterization of HM-lip and TMC-HM-lip

Formulation	Size (nm)	PDI	Zeta potential (mV)	EE (%)
HM-lip	155.0±14.5	0.159±0.018	-18.4±2.7	80.90±0.01
TMC-HM-lip	172.0±15.2	0.188±0.012	16.6±3.5	81.20±0.02

Abbreviations: HM-lip, harmine liposomes; TMC, N-trimethyl chitosan; TMC-HM-lip, TMC-coated harmine liposomes; PDI, polydispersity index; EE, entrapment efficiency.

HM-lip and TMC-HM-lip" section, and the Papp was calculated according to the following equation:

$$P_{app} = \frac{dQ/dt}{AC_0} \quad (3)$$

where dQ/dt is the slope of the cumulative HM amount transported during the time of 2 hours, A is the area of the insert (1.1 cm²), and C_0 is the starting concentration of HM, HM-lip, or TMC-HM-lip.

The TEER of Caco-2 monolayers was measured with a resistance meter during the time course of the study.

Results

Characterization of HM-lip and TMC-HM-lip

The particle sizes, zeta potentials, and entrapment efficiencies of HM-lip and TMC-HM-lip are shown in Table 1. After coating with TMC, the particle size of liposomes increased, but their entrapment efficiency did not change. The zeta potential of HM-lip was negative, whereas that of TMC-HM-lip was positive, indicating that the surface of HM-lip was successfully coated with TMC (Figure 1).²²

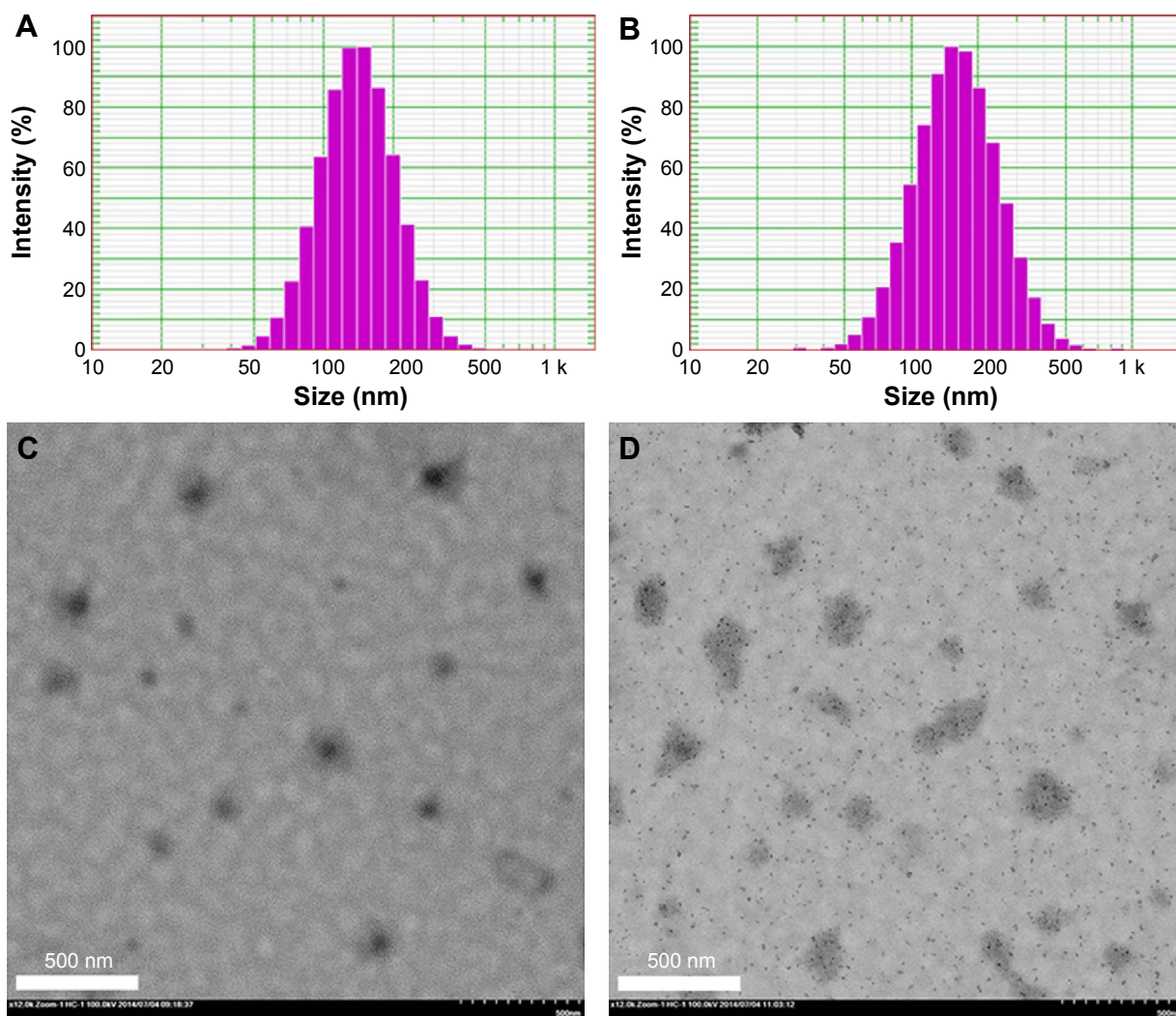


Figure 1 Particle size distribution of HM-lip (A) and TMC-HM-lip (B). TEM of HM-lip (C) and TMC-HM-lip (D).

Abbreviations: HM-lip, harmine liposomes; TMC-HM-lip, TMC-coated harmine liposomes; TMC, N-trimethyl chitosan; TEM, transmission electron microscopy.

Release of HM from HM, HM-lip and TMC-HM-lip in vitro

The release of HM from HM, HM-lip, and TMC-HM-lip solutions in vitro is shown in Figure 2. The release of HM was pH dependent, as indicated by the fast release in low-pH medium and the slow release in high-pH medium. The release of HM from HM-lip and TMC-HM-lip was slower than that from HM solution, particularly in PBS with pH 6.8 and pH 7.4. Hence, HM-lip and TMC-HM-lip exhibited sustained-release capability in the intestines and plasma. Conversely, HM released rapidly from HM-lip and TMC-HM-lip in 0.1 mol/L HCl, because of the improved solubility of HM at lower pH.

In vivo pharmacokinetic studies

The plasma concentration–time curve and pharmacokinetic parameters of HM after administering HM in different formulations intravenous (IV) or intragastric (IG) to rats are shown in Figure 3 and Table 1, respectively. As shown in Figure 3, the elimination rate of HM IG was faster than that of HM-lip IG and TMC-HM-lip IG. The bioavailability of HM through oral administration was lower (29.16%), and that of HM-lip and TMC-HM-lip increased to 50.93% and 73.11%,

respectively. An interesting feature observed in Figure 3 is the presence of double peaks in the plasma concentration–time curve of HM-lip and TMC-HM-lip IG.

Retentive behavior of HM-lip and TMC-HM-lip in GIT

As shown in Figure 4, the gastric emptying of HM solution was so rapid, causing the retention amount in the stomach to decrease by about 10% within 1 hour. The retention amount of HM-lip and TMC-HM-lip was higher than that of HM in the stomach. Moreover, the retention amount of HM, HM-lip, and TMC-HM-lip in the small intestine was lower than that in the stomach, suggesting that HM, HM-lip, and TMC-HM-lip were rapidly absorbed in the small intestine. The total retention amount in the GIT was arranged in the following order: TMC-HM-lip > HM-lip > HM solution. Hence, TMC-HM-lip and HM-lip moved slower than HM in the GIT of mice.

Figure 5 shows that the fluorescence intensity of nude mice given TMC-Dir-lip gastrointestinally was stronger than for those given Dir-lip at almost all time points after oral administration, indicating that TMC-Dir-lip moved slower than Dir-lip in the GIT of nude mice.

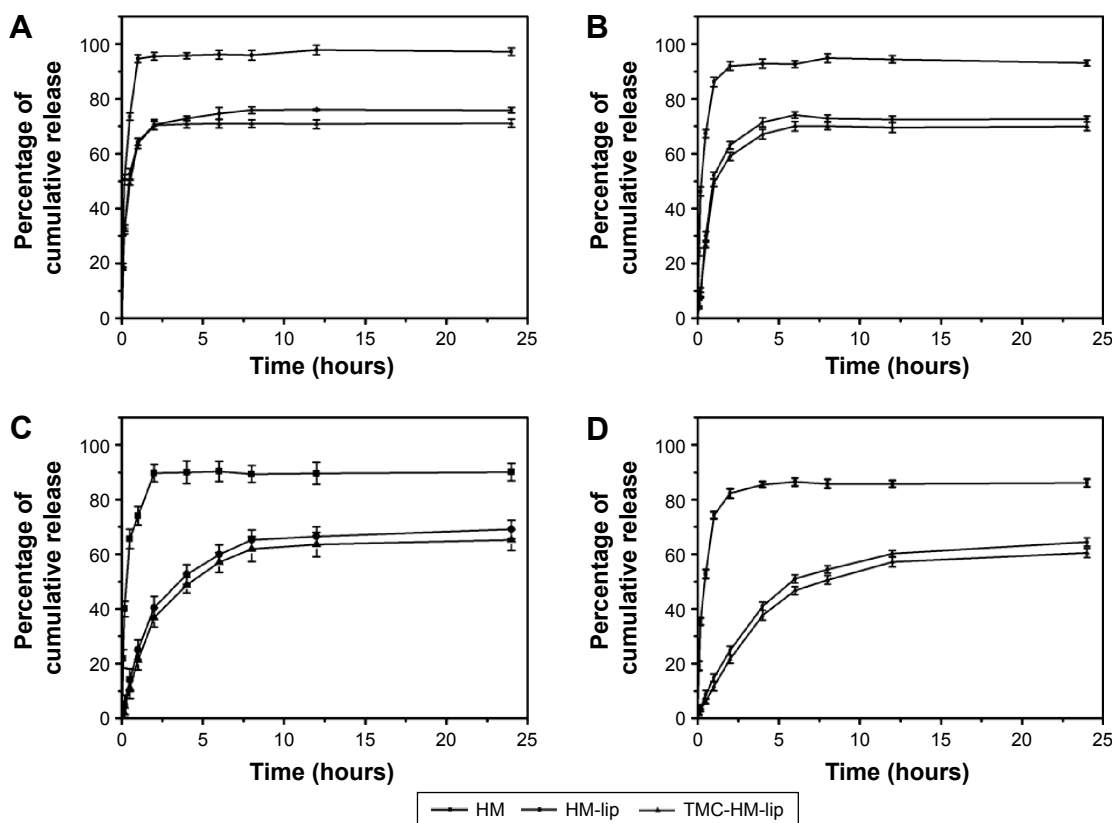


Figure 2 Release of HM from HM, HM-lip, and TMC-HM-lip solution in different release mediums (A) 0.1 M HCl, (B) pH 5.3 PBS, (C) pH 6.8 PBS, and (D) pH 7.4 PBS. $n=3$. **Abbreviations:** HM, harmine; HM-lip, harmine liposomes; TMC, *N*-trimethyl chitosan; TMC-HM-lip, TMC-coated harmine liposomes; PBS, phosphate-buffered saline.

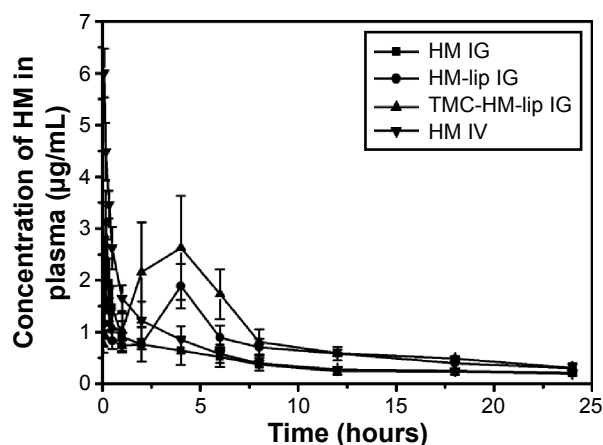


Figure 3 Plasma concentration–time profiles of HM after administration of HM in different formulations to rats through IV or IG (mean \pm SD, $n=5$).

Abbreviations: HM, harmine; IG, intragastric; IV, intravenous; HM-lip, harmine liposomes; TMC, N-trimethyl chitosan; TMC-HM-lip, TMC-coated harmine liposomes; SD, standard deviation.

Toxicity of HM, HM-lip, and TMC-HM-lip to Caco-2 cells

The toxicity of HM, HM-lip, and TMC-HM-lip to Caco-2 cells was evaluated through MTT assay, and the results are shown in Figure 6. The cell viability of Caco-2 cells was

almost 100% after incubation with HM, HM-lip, and TMC-HM-lip solutions at HM concentrations ranging from 10 to 100 $\mu\text{g/mL}$. The cell viability was higher than 90% when treated with HM at 200 $\mu\text{g/mL}$. Hence, HM, HM-lip, and TMC-HM-lip exhibited almost no toxicity to Caco-2 cells at the concentration of 10–200 $\mu\text{g/mL}$.

Degradation of HM, HM-lip, and TMC-HM-lip in Caco-2 cell homogenates

As shown in Figure 7, the degradation of HM in Caco-2 cell homogenates was very rapid resulting in more than 60% of HM being degraded within 120 minutes. Conversely, the degradation of HM-lip and TMC-HM-lip was slower, with more than 80% of drug retained within the same time. Hence, HM-lip and TMC-HM-lip can protect HM from degradation in Caco-2 cell homogenates.

Uptake studies

Effect of time on the uptake of HM, HM-lip, and TMC-HM-lip

As shown in Figure 8, the uptake of HM, HM-lip, and TMC-HM-lip (40 $\mu\text{g/mL}$) into Caco-2 monolayers was

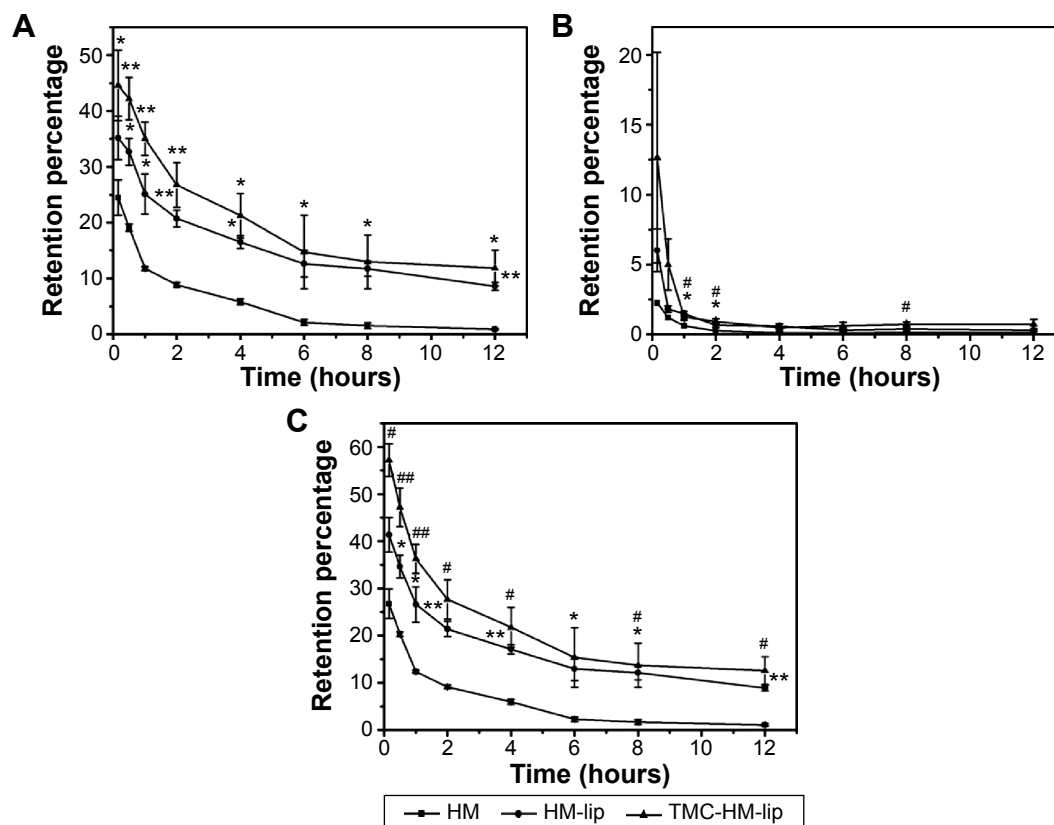


Figure 4 Retentive behavior of HM, HM-lip, and TMC-HM-lip in stomach (A), small intestine (B), and the GIT (C) measured by HPLC ($n=3$).

Notes: * $P<0.05$; ** $P<0.01$, HM-lip versus HM; # $P<0.05$; ## $P<0.01$, TMC-HM-lip versus HM.

Abbreviations: HM, harmine; HM-lip, harmine liposomes; TMC, N-trimethyl chitosan; TMC-HM-lip, TMC-coated harmine liposomes.

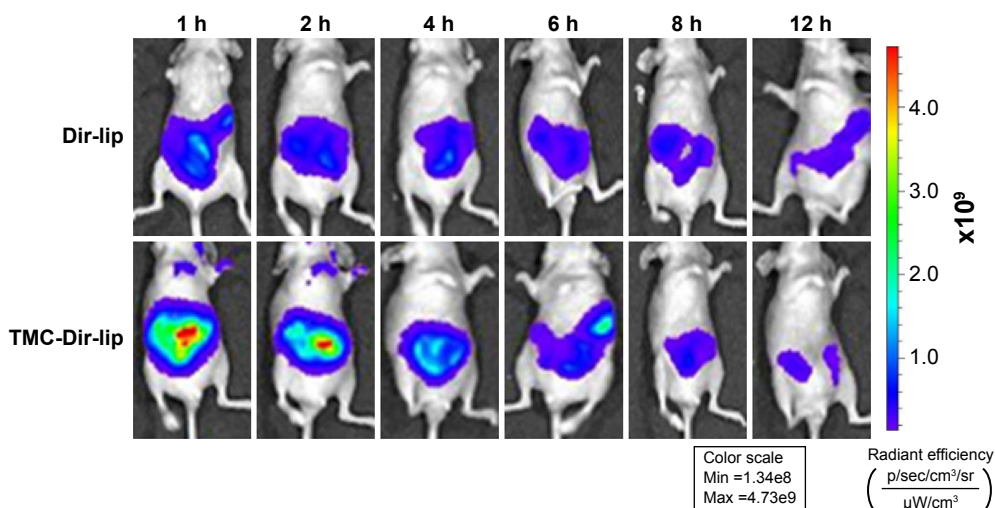


Figure 5 In vivo NIR imaging of nude mice after the administration of Dir-lip and TMC-Dir-lip IG.

Abbreviations: Dir-lip, Dir-loaded liposomes; TMC, *N*-trimethyl chitosan; TMC-Dir-lip, Dir-loaded liposomes coated with TMC; NIR, near-infrared; IG, intragastric.

approximately linear in relation to time at 37°C from 0 to 60 minutes. The uptake of HM was saturated within a shorter time than that of HM-lip and TMC-HM-lip. Considering the optimal absorption rate, cell characteristics, and operational feasibility, 30 minutes was set as the uptake time for the next experiments.

Effect of concentration on the uptake of HM, HM-lip, and TMC-HM-lip

Figure 9 shows the effect of concentration on the uptake of HM, HM-lip, and TMC-HM-lip by Caco-2 cell monolayers. The uptake of HM, HM-lip, and TMC-HM-lip increased as the concentration increased. The uptake of HM was linear in relation to the concentration from 20 to 80 µg/mL at 37°C.

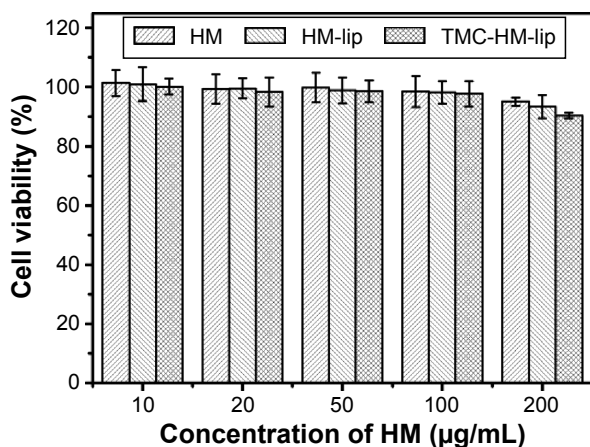


Figure 6 Cell viability of Caco-2 cells treated with HM, HM-lip, and TMC-HM-lip solutions at different concentrations (n=4).

Abbreviations: HM, harmine; HM-lip, harmine liposomes; TMC, *N*-trimethyl chitosan; TMC-HM-lip, TMC-coated harmine liposomes.

As concentrations were increased to 80 µg/mL, the uptake of HM, HM-lip, and TMC-HM-lip showed a saturation phenomenon and was not linear.

Effect of inhibitors

The effects of the energy inhibitor NaN_3 , p-gp inhibitor CyA, and endocytosis inhibitor CPZ on the uptake of HM, HM-lip, and TMC-HM-lip into Caco-2 cells are shown in Figure 10. The uptake of HM-lip and TMC-HM-lip were significantly higher than that of HM when not treated with any inhibitors. The three inhibitors did not affect the uptake of HM. However, the uptake of HM-lip and TMC-HM-lip was increased by NaN_3 and CPZ, but was not affected by

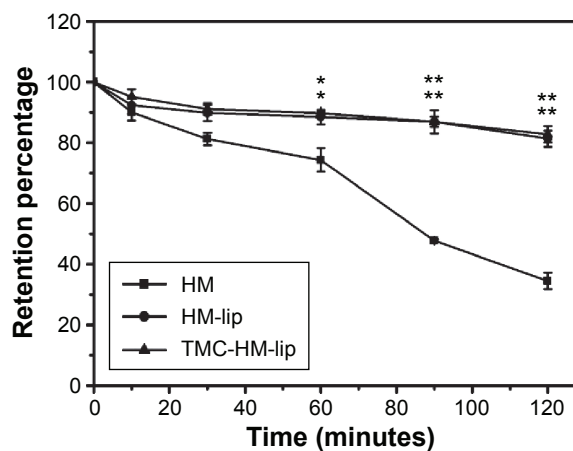


Figure 7 Retention percentage of HM, HM-lip, and TMC-HM-lip after incubation with Caco-2 cell homogenates (n=3).

Note: * $P < 0.05$, ** $P < 0.01$, versus HM.

Abbreviations: HM, harmine; HM-lip, harmine liposomes; TMC, *N*-trimethyl chitosan; TMC-HM-lip, TMC-coated harmine liposomes.

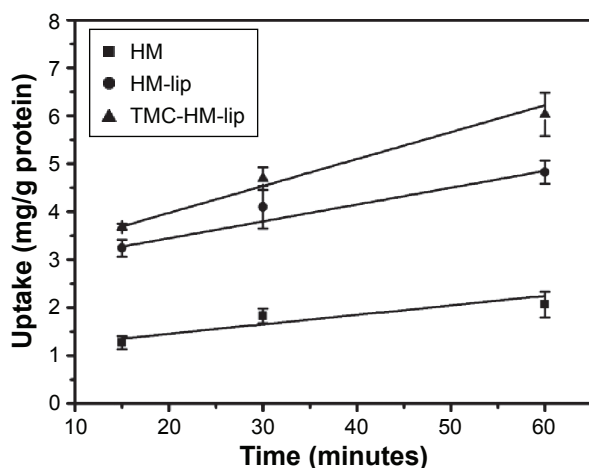


Figure 8 Effect of time on the uptake of HM, HM-lip, and TMC-HM-lip (n=3).
Abbreviations: HM, harmine; HM-lip, harmine liposomes; TMC, N-trimethyl chitosan; TMC-HM-lip, TMC-coated harmine liposomes.

CyA. These results suggested that passive transport was the main uptake mechanism of HM into Caco-2 cells and that endocytosis may be the main uptake mechanism of HM-lip and TMC-HM-lip.

Bidirectional transport of HM, HM-lip, and TMC-HM-lip across Caco-2 cell monolayers

The results of the bidirectional transport of HM, HM-lip, and TMC-HM-lip across the Caco-2 cell monolayers at a dose of 40 $\mu\text{g}/\text{mL}$ at 37°C are shown in Figure 11. TMC-HM-lip and HM-lip could significantly improve the transport of HM from the apical side to the basolateral side, with $P_{\text{app(AL-BL)}}$ increasing from $(5.11 \pm 0.69) \times 10^{-6}$ to $(12.79 \pm 1.617) \times 10^{-6}$ and $(19.12 \pm 1.20) \times 10^{-6}$, respectively. However, the $P_{\text{app(BL-AL)}}$ of

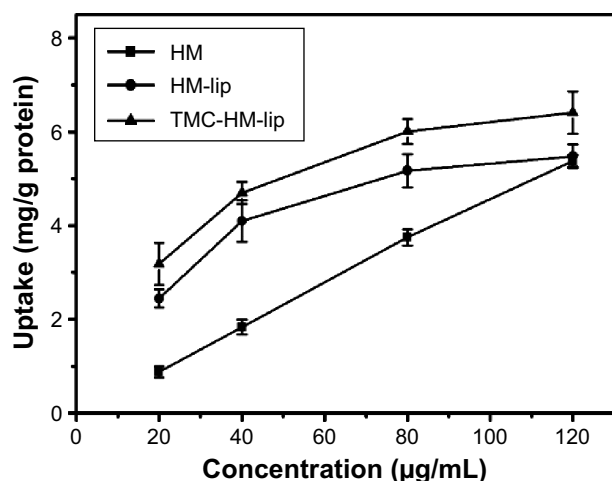


Figure 9 Effect of concentration on the uptake of HM, HM-lip, and TMC-HM-lip (n=3).
Abbreviations: HM, harmine; HM-lip, harmine liposomes; TMC, N-trimethyl chitosan; TMC-HM-lip, TMC-coated harmine liposomes.

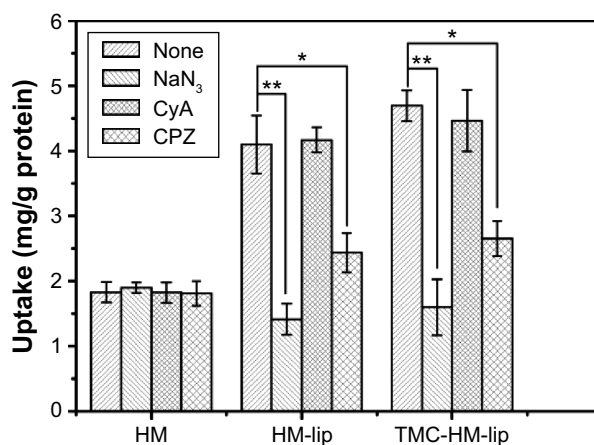


Figure 10 Effect of inhibitors on the uptake of HM, HM-lip, and TMC-HM-lip.
Note: * $P < 0.05$, ** $P < 0.01$, versus control group.
Abbreviations: HM, harmine; HM-lip, harmine liposomes; TMC, N-trimethyl chitosan; TMC-HM-lip, TMC-coated harmine liposomes.

TMC-HM-lip and HM-lip was lower than that of HM. The $P_{\text{app(AL-BL)}}/P_{\text{app(BL-AL)}}$ ratios of TMC-HM-lip (4.97) and HM-lip (3.79) were higher than that of HM (1.27), indicating that TMC-HM-lip and HM-lip improved the absorption of HM.

The TEER values of the Caco-2 monolayers treated with unmodified medium, medium with HM, HM-lip, TMC-HM-lip (40 $\mu\text{g}/\text{mL}$), and TMC (0.1%, w/w) are shown in Figure 12. The TEER of the cell monolayers treated with unmodified medium, medium with HM, or HM-lip minimally decreased by lower than 15%. However, the reduction of TEER was higher than 30% in the cell monolayers treated with TMC-HM-lip. Furthermore, the reduction was high (at about 50%) in the Caco-2 cell monolayers treated with TMC solution. The reduction of TEER resulted from the opening of tight junctions by TMC-HM-lip and TMC.²³

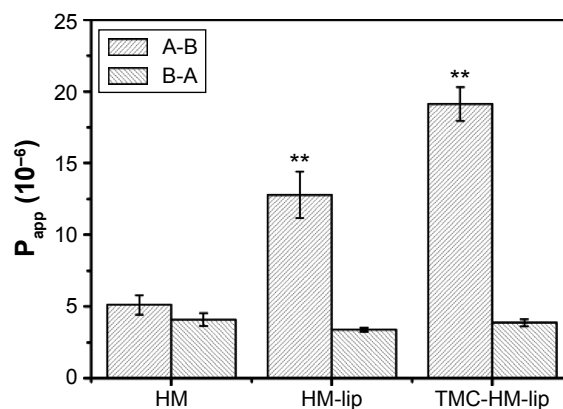


Figure 11 Bidirectional transport of HM, HM-lip, and TMC-HM-lip across Caco-2 cell monolayers (40 $\mu\text{g}/\text{mL}$, 37°C) (n=3).
Note: ** $P < 0.01$, versus HM.
Abbreviations: HM, harmine; HM-lip, harmine liposomes; P_{app} , apparent permeability coefficient; TMC, N-trimethyl chitosan; TMC-HM-lip, TMC-coated harmine liposomes.

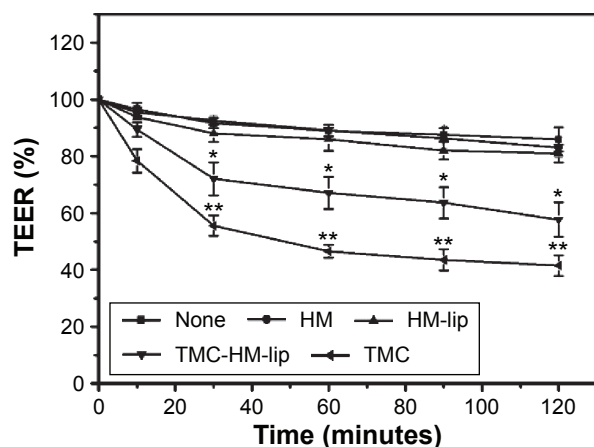


Figure 12 TEER of Caco-2 cell monolayers (n=3) treated with unmodified medium (none), medium with HM, HM-lip, TMC-HM-lip (40 µg/mL), and TMC (0.1%, w/w). **Note:** * $P < 0.05$, ** $P < 0.01$, versus HM.

Abbreviations: HM, harmine; HM-lip, harmine liposomes; TMC, *N*-trimethyl chitosan; TMC-HM-lip, TMC-coated harmine liposomes; TEER, transepithelial electrical resistance.

Discussion

In this study, HM-lip and TMC-HM-lip were prepared. Their release in vitro, pharmacokinetics, retention behavior in the GIT, degradation, uptake, and transport across Caco-2 cell monolayers were studied.

In the degradation test, HM was rapidly degraded in the Caco-2 cell homogenates (Figure 7). As the enzymes in the homogenates were similar to those in intestinal epithelial cells, we could infer that some HM was degraded in the GIT after oral administration. A previous study reported that the *O*-demethylation of HM was catalyzed by CYP1A1 (98.5), CYP1A2 (35), CYP2C9 (16), CYP2C19 (30), and CYP2D6 (115), which may exist in the GIT.²⁴ Degradation in the GIT could be attributed to the first-pass effect and the low oral bioavailability of HM at 25.25%±6.05%. As shown in Figures 9–11, the uptake of HM into Caco-2 cells through passive diffusion mechanism was not dependent on concentration and not affected by energy inhibitors and endocytosis inhibitors.²⁵ Moreover, the uptake of HM into Caco-2 cells was not affected by the efflux effect of p-gp, because it was not increased by CyA. At $P_{app(AL-BL)}$ of HM higher than 10^{-6} , the ratio of $P_{app(AL-BL)}/P_{app(BL-AL)}$ was higher than 1 (Figure 11) and the retention amount of HM in the mouse intestine was low. This finding indicated that HM can be absorbed well in the GIT.

To improve the oral bioavailability of HM, we encapsulated it into liposomes through a thin-film hydration and pH-gradient method and then coated with TMC. For weakly basic drugs, such as doxorubicin and HM, pH-gradient

method was an appropriate method to obtain high encapsulation efficiency when these drugs were encapsulated into liposomes.²⁶ HM-lip could be coated with TMC to prepare TMC-HM-lip via the electrostatic interaction between anionic phospholipids and cationic TMC, resulting in minimal increase in particle size and charge reversal in the zeta potential of HM-lip.²⁷

HM-lip and TMC-HM-lip could protect HM against degradation in Caco-2 cell homogenates (Figure 8), reduce the first-pass effect, and thus improve the oral bioavailability. The uptakes of HM-lip and TMC-HM-lip into Caco-2 cells occurred via the clathrin-mediated endocytic pathway, which can be saturated and affected by endocytosis inhibitors (CPZ) and energy inhibitors (NaN_3) (Figures 9 and 10).²⁸ The uptake amounts of HM-lip and TMC-HM-lip into Caco-2 cells were higher than that of HM if they did not reach the saturation concentration (Figure 9). In consideration of the positive charges, TMC-HM-lip can be easily absorbed and can further improve the uptake of HM-lip. Figure 11 showed that TMC-HM-lip exhibited the highest $P_{app(AL-BL)}$, indicating that TMC-HM-lip can demonstrate the highest transport amount across Caco-2 monolayers and the optimal absorption in the intestines. The optimal absorption of TMC-HM-lip could be attributed to the following: 1) the uptake of TMC-HM-lip was the highest, and some TMC-HM-lip were transported via the transcellular pathway and 2) TMC coated on TMC-HM-lip contributed to the opening of the tight junctions among Caco-2 cell monolayers and some TMC-HM-lip were transported via the paracellular pathway (Figure 12).²⁹ In addition, the longest retention time in the mouse GIT was demonstrated by TMC-HM-lip. Prolonging the retention time of drugs in the GIT can help improve their oral bioavailability (Figures 4 and 5). As a result, the oral bioavailability of TMC-HM-lip (59.53%±12.58%) was higher than that of HM-lip (39.01%±7.69%) and HM (25.25%±6.05%) (Figure 3 and Table 2).

The double peaks observed in the plasma concentration–time curve of HM-lip and TMC-HM-lip IG was a rare phenomenon. These peaks may not be attributed to the effect of enterohepatic circulation, because the plasma concentration–time curve of orally administered HM did not exhibit double peaks. Considering the release in vitro (Figure 2), pharmacokinetics (Figure 3), and retentive behavior of HM, HM-lip, and TMC-HM-lip (Figures 4 and 5), we speculated that the “double-peaks” may be caused by the following: a part of HM was rapidly split from HM-lip and TMC-HM-lip in the GIT and thus rapidly absorbed resulting in the first peak, and then

Table 2 Pharmacokinetic parameters of HM in rats (mean \pm SD, n=5)

Route	Formulation	Dose (mg/kg)	C _{max} (µg/mL)	AUC (µg·h/mL)	BA (%)
IV	HM	20	–	12.88 \pm 1.25	–
	HM	60	3.11 \pm 0.32	9.76 \pm 2.34	25.25 \pm 6.05
IG	HM-lip	60	1.89 \pm 0.43	15.08 \pm 2.97*	39.01 \pm 7.69**
	TMC-HM-lip	60	2.67 \pm 1.05	23.00 \pm 4.86*	59.53 \pm 12.58**

Note: *P<0.05, **P<0.01, versus HM IG.

Abbreviations: HM, harmine; AUC, area under the concentration–time curve; BA, bioavailability; IV, intravenous; IG, intragastric; HM-lip, harmine liposomes; TMC, N-trimethyl chitosan; TMC-HM-lip, TMC-coated harmine liposomes.

another part of HM-lip and TMC-HM-lip transferred into the small intestine from the stomach and was thus absorbed later because of the retention effect in the GIT (mainly in the stomach), resulting in the second peak. As TMC-HM-lip exhibited a stronger retention effect and better absorption, the second peak of TMC-HM-lip was higher than that of HM-lip (Figure 3).

In the retentive behavior test, HM-lip and TMC-HM-lip moved slower than HM in the GIT. HM-lip and TMC-HM-lip were mainly stranded in the stomach; hence, they exhibited delayed gastric emptying.¹⁹ With larger particle sizes and positive zeta potential, TMC-HM-lip presented stronger mucoadhesive and gastroretentive properties and further prolonged the retention time in the GIT. However, the retention amounts of HM-lip and TMC-HM-lip in the small intestine was lower than that in the stomach. As shown in Figure 11, the $P_{app(AL-BL)}$ values of HM-lip and TMC-HM-lip were higher than 10^{-5} , indicating that HM-lip and TMC-HM-lip can be rapidly absorbed by intestinal epithelial cells. These results agreed with the findings of Sugihara et al³⁰ but differ from the findings of Takeuchi et al.³¹ Further in vivo studies must be performed to investigate the sites where liposomes are mainly stranded.

Conclusion

In summary, TMC-HM-lip can prolong the retention time in the GIT, protect HM from enzyme degradation, and improve transport across intestinal epithelial cells, thus enhancing the oral bioavailability of HM.

Acknowledgments

This work was supported by the National Natural Science Foundation projects of China (numbers 81571788 and 81273463), the Jiangsu Science and Technology Support Plan (BE2011670), the National Student and Innovative experimental plan (111028533, microcomputer number: 5731503311), and the Priority Academic Program Development of Jiangsu Higher Education Institutions (PAPD).

Disclosure

The authors report no conflicts of interest in this work.

References

1. Thanki K, Gangwal RP, Sangamwar AT, Jain S. Oral delivery of anti-cancer drugs: challenges and opportunities. *J Control Release*. 2013;170(1):15–40.
2. Liu YT, Hao HP, Xie HG, et al. Extensive intestinal first-pass elimination and predominant hepatic distribution of berberine explain its low plasma levels in rats. *Drug Metab Dispos*. 2010;38(10):1779–1784.
3. Werle M, Takeuchi H. Chitosan–aprotinin coated liposomes for oral peptide delivery: development, characterisation and in vivo evaluation. *Int J Pharm*. 2009;370(1):26–32.
4. Roger E, Lagarce F, Garcion E, Benoit JP. Biopharmaceutical parameters to consider in order to alter the fate of nanocarriers after oral delivery. *Nanomedicine*. 2010;5(2):287–306.
5. Niu M, Lu Y, Hovgaard L, et al. Hypoglycemic activity and oral bioavailability of insulin-loaded liposomes containing bile salts in rats: the effect of cholate type, particle size and administered dose. *Eur J Pharm Biopharm*. 2012;81(2):265–272.
6. Makhlof A, Fujimoto S, Tozuka Y, Takeuchi H. In vitro and in vivo evaluation of WGA–carbopol modified liposomes as carriers for oral peptide delivery. *Eur J Pharm Biopharm*. 2011;77(2):216–224.
7. Panya A, Laguerre M, Lecomte J, et al. Effects of chitosan and rosamarinate esters on the physical and oxidative stability of liposomes. *J Agric Food Chem*. 2010;58(9):5679–5684.
8. Garcia-Fuentes M, Alonso MJ. Chitosan-based drug nanocarriers: where do we stand? *J Control Release*. 2012;161(2):496–504.
9. Amidi M, Mastrobattista E, Jiskoot W, Hennink WE. Chitosan-based delivery systems for protein therapeutics and antigens. *Adv Drug Deliv Rev*. 2010;62(1):59–82.
10. Li N, Zhuang CY, Wang M, Sui CG, Pan WS. Low molecular weight chitosan-coated liposomes for ocular drug delivery: in vitro and in vivo studies. *Drug Deliv*. 2012;19(1):28–35.
11. Diebold Y, Jarrin M, Sáez V, et al. Ocular drug delivery by liposome–chitosan nanoparticle complexes (LCS-NP). *Biomaterials*. 2007;28(8):1553–1564.
12. Artursson P, Palm K, Luthman K. Caco-2 monolayers in experimental and theoretical predictions of drug transport. *Adv Drug Deliv Rev*. 2012;64:280–289.
13. Zhang H, Sun K, Ding J, et al. Harmine induces apoptosis and inhibits tumor cell proliferation, migration and invasion through down-regulation of cyclooxygenase-2 expression in gastric cancer. *Phytomedicine*. 2014;21(3):348–355.
14. Guan M, Zhou Y, Zhu QL, et al. N-trimethyl chitosan nanoparticle-encapsulated lactosyl-norcantharidin for liver cancer therapy with high targeting efficacy. *Nanomedicine*. 2012;8(7):1172–1181.
15. Guo P, You JO, Yang J, Moses MA, Auguste DT. Using breast cancer cell CXCR4 surface expression to predict liposome binding and cytotoxicity. *Biomaterials*. 2012;33(32):8104–8110.

16. Bei YY, Zhou XF, You BG, et al. Application of the central composite design to optimize the preparation of novel micelles of harmine. *Int J Nanomedicine*. 2013;8:1795.
17. Takeuchi H, Matsui Y, Sugihara H, Yamamoto H, Kawashima Y. Effectiveness of submicron-sized, chitosan-coated liposomes in oral administration of peptide drugs. *Int J Pharm*. 2005;303(1):160–170.
18. Du D, Chang N, Sun S, et al. The role of glucose transporters in the distribution of *p*-aminophenyl- α -D-mannopyranoside modified liposomes within mice brain. *J Control Release*. 2014;182(1):99–110.
19. Lin IC, Liang M, Liu TY, Ziora ZM, Monteiro MJ, Toth I. Interaction of densely polymer-coated gold nanoparticles with epithelial Caco-2 monolayers. *Biomacromolecules*. 2011;12(4):1339–1348.
20. Li H, Song JH, Park JS, Han K. Polyethylene glycol-coated liposomes for oral delivery of recombinant human epidermal growth factor. *Int J Pharm*. 2003;258(1):11–19.
21. Guan M, Zhu QL, Liu Y, et al. Uptake and transport of a novel anticancer drug-delivery system: lactosyl-norcantharidin-associated *N*-trimethyl chitosan nanoparticles across intestinal Caco-2 cell monolayers. *Int J Nanomedicine*. 2012;7:1921.
22. Chen H, Wu J, Sun M, et al. *N*-trimethyl chitosan chloride-coated liposomes for the oral delivery of curcumin. *J Liposome Res*. 2012;22(2):100–109.
23. Yeh TH, Hsu LW, Tseng MT, et al. Mechanism and consequence of chitosan-mediated reversible epithelial tight junction opening. *Biomaterials*. 2011;32(26):6164–6173.
24. Yu AM, Idle JR, Krausz KW, K pfer A, Gonzalez FJ. Contribution of individual cytochrome P450 isozymes to the *O*-demethylation of the psychotropic β -carboline alkaloids harmaline and harmine. *J Pharmacol Exp Ther*. 2003;305(1):315–322.
25. Khan SI, Abourashed EA, Khan IA, Walker LA. Transport of harman alkaloids across Caco-2 cell monolayers. *Chem Pharm Bull (Tokyo)*. 2004;52(4):394–397.
26. Gubernator J. Active methods of drug loading into liposomes: recent strategies for stable drug entrapment and increased in vivo activity. *Expert Opin Drug Deliv*. 2011;8(5):565–580.
27. Mertins O, Schneider PH, Pohlmann AR, da Silveira NP. Interaction between phospholipids bilayer and chitosan in liposomes investigated by ³¹P NMR spectroscopy. *Colloids Surf B Biointerfaces*. 2010;75(1):294–299.
28. Zuhorn IS, Kalicharan R, Hoekstra D. Lipoplex-mediated transfection of mammalian cells occurs through the cholesterol-dependent clathrin-mediated pathway of endocytosis. *J Biol Chem*. 2002;277(20):18021–18028.
29. Huang A, Makhlof A, Ping Q, Tozuka Y, Takeuchi H. *N*-trimethyl chitosan-modified liposomes as carriers for oral delivery of salmon calcitonin. *Drug Deliv*. 2011;18(8):562–569.
30. Sugihara H, Yamamoto H, Kawashima Y, Takeuchi H. Effects of food intake on the mucoadhesive and gastroretentive properties of submicron-sized chitosan-coated liposomes. *Chem Pharm Bull (Tokyo)*. 2012;60(10):1320–1323.
31. Takeuchi H, Matsui Y, Yamamoto H, Kawashima Y. Mucoadhesive properties of carbopol or chitosan-coated liposomes and their effectiveness in the oral administration of calcitonin to rats. *J Control Release*. 2003;86(2):235–242.

International Journal of Nanomedicine

Publish your work in this journal

The International Journal of Nanomedicine is an international, peer-reviewed journal focusing on the application of nanotechnology in diagnostics, therapeutics, and drug delivery systems throughout the biomedical field. This journal is indexed on PubMed Central, MedLine, CAS, SciSearch®, Current Contents®/Clinical Medicine,

Submit your manuscript here: <http://www.dovepress.com/international-journal-of-nanomedicine-journal>

Dovepress

Journal Citation Reports/Science Edition, EMBase, Scopus and the Elsevier Bibliographic databases. The manuscript management system is completely online and includes a very quick and fair peer-review system, which is all easy to use. Visit <http://www.dovepress.com/testimonials.php> to read real quotes from published authors.